The Application of Artificial Intelligence in Combustion Diagnosis Systems in Thermal Power Plants

Tao Jia

tjcoch[at]outlook.com

Abstract: ***The application of artificial intelligence in thermal power plants is discussed. Digital image processing, fuzzy logic and time-series analysis are often employed to conduct the diagnosis of the combustion in the furnaces in thermal power plants. The connection between radiation heat transfer and digital image processing makes the accurate visualization of the temperature of the flame of the combustion possible, and rich information on combustion can be obtained from the texture of the flame images. Fuzzy logic provides a mathematical framework to measure the situation where uncertainty exists, and it takes the best possible decision based on the input information. Time series analysis gives a qualitative way to measure the recorded historical data of the textures of the flame images and it can be used to predict the future trend of the combustion.***

Keywords: artificial intelligence; image processing; fuzzy logic; time-series analysis; combustion; flame; thermal power plant

1. Introduction

The employment of advanced diagnosis systems to diagnose the combustion in the furnaces in thermal power plants is crucial to optimize the supply of fuel and oxygen, save energy, and enhance the safety of the thermal power plants. Artificial intelligence has been widely used in industry [1-3]. A system based on artificial intelligence is very sensitive to the change of its environment and can timely maximize its chance to achieve its goals with minimum cost. Research on combustion and flame [4-9]plays an important role in optimizing energy utilization in thermal power plants. Combustion diagnosis based on flame image processing is a convincing example that artificial intelligence can be successfully applied to improve the performance of thermal power plants.

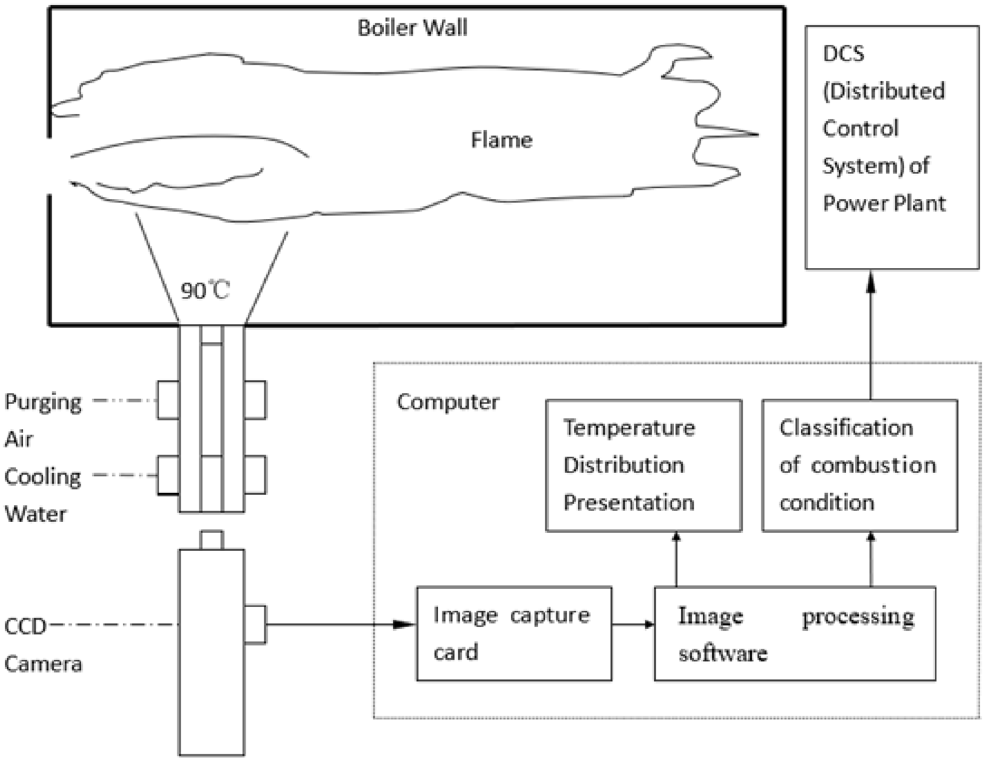

Figure 1: The configuration of combustion flame image processing system

In Figure 1, it shows the configuration of the combustion diagnosis system based on flame image processing technology. A CCD camera is employed to capture the flame images and transfer it into the computer. A computer program is used to conduct the flame image processing and extract the textures of the flame images to realize the classification of the combustion conditions such as oxygen-rich, oxygen-lean, and stoichiometric. Finally, the signal of the combustion state is sent to the distributed control system of the power plant to optimize the control strategy.

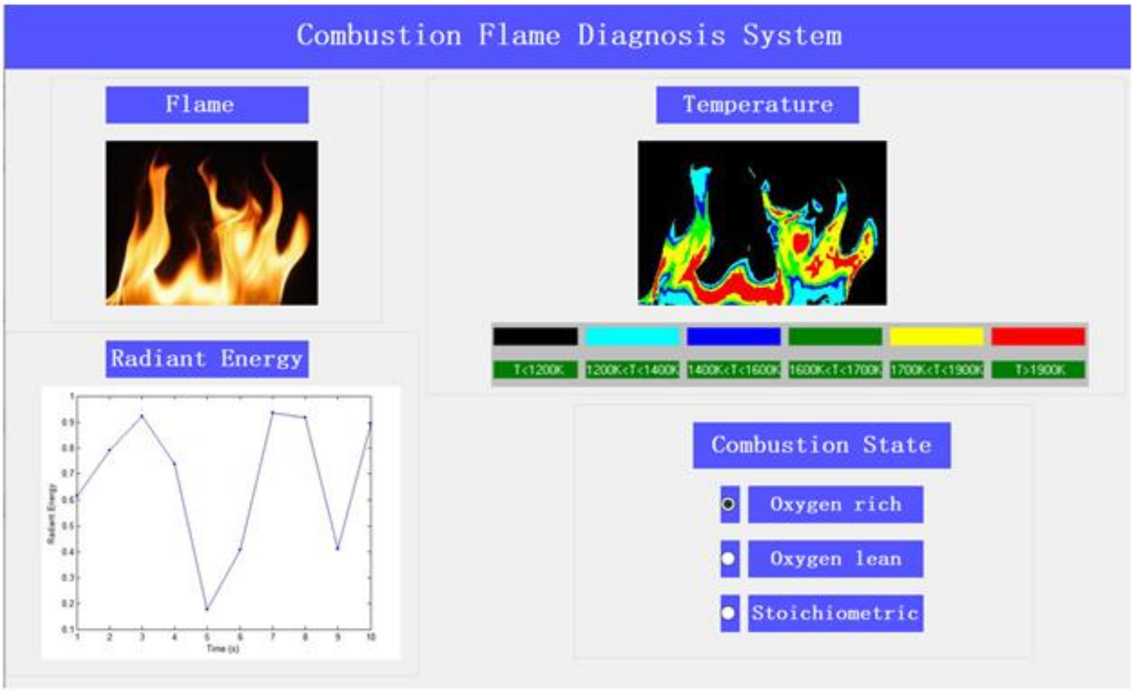

Figure 2: The interface of the computer software of combustion flame image processing system

In Figure 2, the interface of the computer software foe the combustion diagnosis is shown. The contents include original flame image, temperature distribution inside the flame, the radiant energy of the flame, and the combustion state. The textures [10] of the images usually include the average values of the pixels, the standard deviation of the values of the pixels, the skewness of the values of the pixels, the Shannon entropy of the values of the pixels, and the threshold value based on Otsu's method which is used to separate the region of the flame and the region of the background. The time-series [11] data of these textures is stored to be analyzed to find some patterns of the change of the combustion state. And the judgement of the combustion state is often based on fuzzy logic [10]. The typical membership functions include the triangular, trapezoidal, piecewise linear, Gaussian, and Singleton.

The principle of calculating the flame temperature based on flame image is introduced below. The wavelength and temperature concerned in the study of coal combustion range from 300nm to 1000nm and from 800K to 2500K, respectively. Within these ranges, Planck's law can be replaced by Wien's law [12] :

$$E(\lambda,T)=\varepsilon_{\lambda}\frac{C_1}{\lambda^5}\exp(-\frac{C_2}{\lambda T}) \quad (1)$$

Where $E(\lambda,T)$ is the monochromatic exitance, T is the absolute temperature, ε_{λ} is monochromatic emissivity, λ is the wavelength of the radiation, C_1 and C_2 are the first and second Plank's constants.

Considering a radiation point with temperature of T emitting a red monochromatic light with wavelength λ_R, monochromatic exitance $E(\lambda_R,T)$, monochromatic emissivity of $\varepsilon_{\lambda.R}$ and a green monochromatic light with wavelength λ_G, monochromatic exitance $E(\lambda_G,T)$, monochromatic emissivity of $\varepsilon_{\lambda.G}$.

According to Wien's law:

$$E(\lambda_R,T)=\varepsilon_{\lambda.R}\cdot\frac{C_1}{\lambda_R{}^5}\exp(-\frac{C_2}{\lambda_R T}) \quad (2)$$

$$E(\lambda_G,T)=\varepsilon_{\lambda.G}\cdot\frac{C_1}{\lambda_G{}^5}\exp(-\frac{C_2}{\lambda_G T}) \quad (3)$$

Dividing Eq(2) by Eq(3) results in:

$$\frac{E(\lambda_R,T)}{E(\lambda_G,T)}=\frac{\varepsilon_{\lambda.R}}{\varepsilon_{\lambda.G}}\cdot\left(\frac{\lambda_G}{\lambda_R}\right)^5.\exp\left(\frac{C_2}{\lambda_G T}-\frac{C_2}{\lambda_R T}\right) \quad (4)$$

Rearranging Eq. 4 yields the temperature of the radiation point:

$$T=C_2(\frac{1}{\lambda_G}-\frac{1}{\lambda_R})/\left(\ln\frac{\varepsilon_{\lambda.R}}{\varepsilon_{\lambda.G}}+\ln\frac{E(\lambda_R,T)}{E(\lambda_G,T)}+\ln\left(\frac{\lambda_R}{\lambda_G}\right)^5\right) \quad (5)$$

In flame image processing, a fundamental assumption is that each pixel of a color flame picture can be considered a radiation point, which emits three kinds of monochromatic lights (that are Red, Green and Blue monochromatic lights).

There are large numbers of pixels in a color flame image. Each of the pixels, with 256 grey levels (0-255), has three components: R, G, B (R is the red component (0-255), G is the green component (0-255), B is the blue component (0-255)).

In the coal combustion flame study, it can be considered that R is proportional to red monochromatic light radiant energy at its representative wavelength of 600 nm, G is proportional to green monochromatic light radiant energy at its representative wavelength of 525 nm, and B is proportional to blue monochromatic light radiant energy of at its representative wavelength of 455 nm.

So, for an optional pixel of a color flame picture, its corresponding temperature T(pixel) can be calculated according to Eq. (5) by substituting $\frac{R}{G}$ for $\frac{E(\lambda_R,T)}{E(\lambda_G,T)}$ and considering $\frac{\varepsilon_{\lambda.R}}{\varepsilon_{\lambda.G}} \approx 1$ by ignoring the differences between the corresponding spectral emissivities:

$$T(pixel) = C_2\left(\frac{1}{\lambda_G} - \frac{1}{\lambda_R}\right) / \left(\ln \frac{R}{G} + \ln \left(\frac{\lambda_R}{\lambda_G}\right)^5 \right) \quad (6)$$

where λ_G =525nm, λ_R =600nm, C_2=0.014387m.k, R and G are the pixel's red component and green component, respectively.

For example, for a pixel of a color flame image with RGB=(216, 50, 65), its corresponding temperature can be calculated according to Eq. (6):

$$T(pixel) = 0.0014387\left(\frac{1}{525\times10^{-10}} - \frac{1}{600\times10^{-10}}\right) / \left(\ln \frac{216}{50} + \ln \left(\frac{600}{525}\right)^5 \right) = 1667.87K \quad (7)$$

It is known from Eq (6) that flame temperature field can be obtained after calculating all values of the temperatures corresponding to all pixels.

References

[1] Y. P. Tsang, C. K. M. Lee, Artificial intelligence in industrial design: A semi-automated literature survey, Engineering Applications of Artificial Intelligence, 112, 2022.
[2] P. Rajendra, M. Kumari, M. Dahiya, Impact of artificial intelligence on civilization: Future perspectives, Materials Today: Proceedings, 56, 2022.
[3] K. K. Ramachandran, A. Apsara, S. Mary, J. R. Pitroda, Machine learning and role of artificial intelligence in optimizing work performance and employee behavior, Materials Today: 51, 2022.
[4] U. Jin, K. T. Kim, Influence of radial fuel staging on combustion instabilities and exhaust emissions from lean-premixed multi-element hydrogen/methane/air flames, Combustion and Flame, 242, 2022.
[5] T. Lee, K. T. Kim, High-frequency transverse combustion instabilities of lean-premixed multislit hydrogen-air flames, Combustion and Flame, 238, 2022.
[6] O. A. Zargar, Improving combustion performance of swirling double-concentric jets flames with rich equivalence ratios, Case Studies in Thermal Engineering, 20, 4, 2020.
[7] T. Ohta, Y. Onishi,. Sakai, Modulation of wall turbulence by propagating flame of premixed hydrogen–air combustion, Combustion and Flame, 241, 2022.
[8] D. Ciria, M. P. Orihuela, P. M. Naranjo, R. Chacartegui, J.R. Rico, J. A. Becerra, Flame confinement in biomass combustion systems for particles abatement, Energy Conversion and Management, 264, 2022.
[9] B. Alabaş, Effect of biogas addition on combustion instability of propane flame at different external acoustic enforcement frequencies, Fuel, 317, 2022.
[10] R. C. Gonzalez, R. E. Woods, Digital Image Processing, Prentice-Hall, Inc. 2002.
[11] H. Kantz, T. Schreiber, Nonlinear Time Series Analysis Cambridge University Press, 2003.
[12] J. P. Holman, Heat Transfer, The McGraw-Hill Companies, Inc, 2010.